

**IDENTIFICATION OF DIFFERENTIALLY EXPRESSED
TRANSCRIPTS OF *Tdrd7* NULL MUTANT
MOUSE LENS**

by

Shaili D. Patel

A thesis submitted to the Faculty of the University of Delaware in partial fulfillment of the requirements for the degree of Degree in Biological Sciences in Arts and Sciences with Distinction

Spring 2014

Copyrights 2014 Shaili D. Patel

All Rights Reserved

**IDENTIFICATION OF DIFFERENTIALLY EXPRESSED
TRANSCRIPTS OF *Tdrd7* NULL MUTANT
MOUSE LENS**

by

Shaili D. Patel

Approved: _____
Dr. Salil A. Lachke, PhD.,
Professor in charge of thesis on behalf of the Advisory Committee

Approved: _____
Dr. Jeffery L. Caplan, PhD.,
Committee member from the Department of Delaware Biotechnology
Institute

Approved: _____
Dr. Rolf Joerger, PhD.,
Committee member from the Board of Senior Thesis Readers

Approved: _____
Michelle Provost-Craig, Ph.D.
Chair of the University Committee on Student and Faculty Honors

ACKNOWLEDGMENTS

First and foremost, I would like to thank Dr. Lachke, without whom this project would've been impossible. Thank you soooo much Dr. Lachke, I really hope I can be ten percent of what you are as a person. Additionally, I want to thank you for making such a big difference in my career, I am very thankful for that.

Thank you mom and daddy for the roots and wings. Thank you Parth for being there every single day when I was finishing up my experiments and thesis, you were a great mental support and for being such a good friend.

I would specially like to thank Carrie Barnum, who trained me in this lab. I will be taking all these lab skills to where I go in future, thanks a ton for that Carrie, and thank you for the little treats every once in a while; they were a great power booster ☺. I would also like to thank Archana Siddam, my lab mom. Without you Arch, you know how different things would've been. I am going to miss you so much. I would specially like to thank Anne for helping me with my thesis, without you this thesis writing would not have been possible. You were an awesome Lab Manager; I don't think any of us could've asked for better. Christine, the lab squirrel we made it through the senior year, Cheers! And Smriti, her giggles are funnier than her jokes (but one can laugh either ways, so it works). Last, but not the least, I would like to thank Soma, Deepti, and Sylvie too for the fun times we had together while working in the lab. It was a great experience doing something that I love to do because of the friendly environment with amazing people in my lab. Love you all and I am going to miss you guys a lot!!!

TABLE OF CONTENTS

LIST OF TABLES.....	v
LIST OF FIGURES.....	vi
ABSTRACT.....	ix
1 Lens Function and Homeostasis	1
1.1 Function of the lens	1
1.2 Structure of the lens	2
1.4 Cataracts: Definition and statistics	5
1.5 Regulation of lens development	7
1.6 <i>iSyTE</i> a tool for lens gene discovery	10
1.7 <i>TDRD7</i>	11
1.8 Function of Tudor domain proteins in development and disease	12
1.9 <i>Tdrd7</i> deficiency and spermatogenesis defect	13
1.10 <i>Tdrd7</i> deficiency causes eye disease	13
1.11 <i>Tdrd7</i> lens specific RNA granules (RG)	17
1.12 Regional co-localization with <i>Stau1</i>	18
Methods and Materials	20
2.1 Animals	20
2.2 DNA Isolation from Mouse Tails	20
2.3 Mouse Genotyping by PCR	21
2.4 Agarose Gel Electrophoresis	22
2.5 Isolation of Embryos	23
2.6 Cryostat	24
2.7 Laser Capture Microdissection (LCM)	25
2.8 RNA isolation	26
2.9 cDNA synthesis for Reverse Transcriptase-PCR	28
2.10 Reverse Transcriptase-PCR (RT-PCR)	28
2.11 Primer design	28
Results	32
3.1 Laser Capture Microdissection	32
3.2 RNA isolation from LCM captured tissue	33
3.3 RT-PCR on LCM captured lens tissue	34
Discussion	37

LIST OF TABLES

Table 1: Primers used for amplification of reverse-transcribed mRNAs originating from genes of interest.	29
Table 2: Genes and their function in the lens	30
Table 3: Total number of samples collected by LCM from the apical and basal lens fiber cell regions from <i>Tdrd7</i> ^{-/-} and <i>Tdrd7</i> ^{+/-} mouse lens tissue.....	33
Table 4: RNA concentrations of samples from different regions of the fiber cells.....	34

LIST OF FIGURES

Figure 1: Structure of the human eye. Light passes through the cornea and the lens before being focused on the retina. Located in the anterior of the eye is the cornea (1), posterior to the cornea is the lens (2), which helps to further focus light onto the retina (3). Specialized cells called photoreceptors within the retina then relay the signal to the brain through the optic nerve (4), allowing us to see [43].2

Figure 2: Structure of the mature lens. Cell division occurs in active mitotic regions of the anterior epithelium, and cells move laterally until they invert in the bow region of the lens. They then begin to differentiate into fiber cells that elongate, move toward the center of the cells where they meet with similarly migrated fiber cells but from the opposite end, and interact with them to form sutures [44]....3

Figure 3: Lens development in mammals. In mouse, at embryonic day E9.5 the optic vesicle (OV) induces the surface ectoderm to form the lens placode (LP). The lens placode and the optic vesicle then develop coordinately to form the lens pit (LPT) and the optic cup (OC), respectively. At E10.5, the lens pit closes to form the lens vesicle (LV), which pinches off from the surface ectoderm that contributes to the formation of the cornea (C). At E11.5, epithelial cells located at the anterior part of the vesicle constitute the anterior epithelium (AE). At E11.5, epithelial cells that are located in the posterior part of the lens vesicle initiate differentiation into primary fiber (PF) cells that begin to elongate and fill up the lens vesicle. The lens vesicle is completely filled up by E13.0. Cells of the anterior epithelium differentiate into secondary fiber (SF) cells then elongate, differentiate and lose their organelles and pack tightly around the primary fiber cells. Differentiation of anterior epithelium cells into secondary fiber cells occurs throughout the life of the organism and is necessary to maintain lens transparency [46].5

Figure 4: An example of how cataracts impair vision. The left image is an example of normal vision; the middle and right images are examples of progressively impaired vision as the clouding of the lens progresses [47].7

Figure 5: Vertebrate Ocular development. (a) The anterior neural plate contains the presumptive retinal ectoderm (PRE) (red) surrounded by the neural crest cells (NCCs) (yellow), preplacodal region (PPR) (green), and the epidermis (EPI) (white). (b) The closure of neural tube (NT), leads to the bilateral development of diencephalon into the optic vesicles, which comes in contact with the presumptive lens ectoderm (PLE) on either sides. (c) PLE forms into the lens placode by coordinate signaling; at the same time the optic vesicle invaginates to form the optic cup. (d) The lens placode invaginates and forms the lens pit that detaches from the surface ectoderm to form the lens vesicle. At this stage, the neural retina and retinal pigment epithelium (RPE) are formed by the initiation of optic vesicle invagination. (e) This shows that the adult vertebrate eye has multiple compartments.8

Figure 6: *iSyTE*: integrated Systems Tool for Eye gene discovery, uses mouse embryonic lens gene expression dataset as a bioinformatics filter to select candidate genes from human or mouse genomic regions implicated in disease and to prioritize them for further mutational and functional analyses [26].11

Figure 7: *TDRD7* (Tudor domain containing 7). *TDRD7* has three OST-HTH domains and three Tudor domains, predicted to interact with RNA and methylated arginine residues within other proteins, respectively.12

Figure 8: *TDRD7* mutations in human pediatric cataract. (A) Cataract in DGAP186 (left eye, white arrowhead). (B) Ideogram of normal and inverted chromosome 9 [inv (9)]. Red lines show inversion breakpoints, with a schematic below of the *TDRD7* gene and the resulting change in protein. Dotted black lines marks breakpoints that disrupt *TDRD7* within the 2.6-kb region shown and in *TDRD7* protein. The black bar indicates *TDRD7* genomic probe in Southern analysis. *TaqI* and *StuI* refer to the fragments resulting from restriction enzyme digest. The red bar indicates fosmid clone G248P8912G10 used as a *TDRD7*-specific probe. Purple boxes indicate exons. (C) Chromosomal spread of DGAP186 lymphoblastoid cells analyzed by fluorescence in situ hybridization shows split *TDRD7*-specific red probe, whereas green anchor probe remains intact in inv (9). (D) *TDRD7* haploinsufficiency is demonstrated by Western blot of DGAP186 lymphoblastoid cells. (E) Pedigree of consanguineous family F3R with congenital cataract (solid symbols, affected status; half-solid symbols, carrier status). (F) Sequence chromatogram shows c.1852_1854del (p.617delVal) mutation (boxed) in family F3R [27].15

Figure 9: *TDRD7* Deficiency in human, mouse and chicken causes' cataract [27]. ...16

Figure 10: Lens defects in *Tdrd7* mouse mutant. (A) The histology of control lens at 3 months shows no ocular abnormality while (B) *Tdrd7* Null lens exhibit a severe cataract at the same age. Arrowhead points towards vacuole and the arrow indicates lens mass and the arrow shows capsule rupture.17

Figure 11: At E11.5, TDRD7 and STAU1 expression shows a high degree of co-localization (yellow) in the anterior portion of the FC compartment. DAPI-stained nuclei are blue. (Inset) Higher magnification demonstrates high degree of colocalization (yellow) of TDRD7-RGs and STAU1-RNPs [27].....19

Figure 12: The band sizes were determined both for Het (195bp, lower band in the gel) and KO (500bp, upper band in the gel) DNA samples, respectively.23

Figure 13: Laser Capture Microdissection (LCM) microscope and technology. (A) The inverted P.A.L.M. Laser Capture Microdissection. (B) Schematic of selected regions defocuses and catapults the sample into the 0.5-ml P.A.L.M. adhesive cap held above by a robo mover. (DBI, University of Gothenburg, CCI).26

Figure 14: RT-PCR analysis of LCM captured apical and basal lens tissue. RT-PCR analysis exhibits that *Gapdh*, housekeeping marker, and *Foxe3*, a lens epithelial marker, were expressed equally throughout the apical and basal fiber cells for both *Tdrd7* null and control lens tissue. However, the expression of *Prox1* was considerably low in the *Tdrd7* null basal fiber cells in the lens.....35

Figure 15: Heterozygous apical and basal samples were tested for *Cryaa*, *Cryab*, *Crybal*, *Crybb1*, and, *Cryga*. *Cryaa* was found to be expressed at higher levels in the apical region of the *Tdrd7* heterozygous lens fiber cells compared to the basal region. *Cryab*, *Crybal*, *Crybb1*, and, *Cryga* were found to be expressed at comparable levels in both, apical and basal regions of the *Tdrd7* heterozygous lens fiber cells.36

ABSTRACT

The ocular lens is a transparent tissue within the eye that focuses light on the retina and facilitates high-resolution vision. Cataract is an eye disease that results due to the loss of lens transparency and causes severely impaired vision. It can be caused by genetic perturbations, aging or physiological conditions like diabetes. Cataract treatment depends upon the patient's specific visual needs and often involves surgery. Over 77 million individuals are affected worldwide, and in the United States alone, costs exceed \$3 billion annually. Recently, a mutation in the human *TDRD7* (Tudor domain containing protein 7) gene was shown to cause congenital/pediatric cataracts in patients. Moreover, it was also demonstrated that *Tdrd7* targeted germline knockout or ENU-induced knockout mouse mutants exhibit cataracts that closely resemble the human phenotype. Previous data shows that Tdrd7 protein co-localized with another RNA binding protein termed Stau1 that is involved in localization of mRNA within specific regions in cells. My research goal was to understand the regulatory function of Tdrd7 in the lens. Specifically, I investigated if different RNAs were localized in the apical and the basal regions of differentiating lens fiber cells and if Tdrd7 deficiency affects these mRNA profiles. To achieve this I expanded the *Tdrd7* germline knockout mouse mutant colony and collected *Tdrd7* mutant and control (*Tdrd7*^{+/-} mice that do not exhibit cataracts) embryonic lens tissue for analysis. To study the expression of mRNAs in different locations within fiber cells, I undertook standardization of an approach using Laser Capture Microdissection (LCM). LCM on embryonic lens sections from *Tdrd7* null mutants and control were used to isolate the apical and the basal fiber cell regions at mouse embryonic stage E12.5. Once the specific tissues were collected,

expression of mRNAs was tested by reverse transcriptase combined with polymerase chain reaction (RT-PCR) analysis. In future, microarray or RNA-sequencing based comparative analysis of gene expression profiles of the apical and basal tissues from *Tdrd7* null mutant and control will allow a comprehensive identification of majority of transcripts that are misregulated in these distinct regions as a result of *Tdrd7* mutation.

Chapter 1

Lens Function and Homeostasis

1.1 Function of the lens

The eye is a complex organ with several distinct components and tissue types that function together to render us with the critical sense of sight. Visual information is gathered by refracting light through the cornea and the lens onto the retina. Specialized cells within the retina then relay the signal through the optic nerve to the brain, which interprets the image. Importantly, the lens contributes about 33% of the refractive power of the eye in the process of vision [42]. In order for the lens to maintain such a high refractive index, it needs to remain transparent.

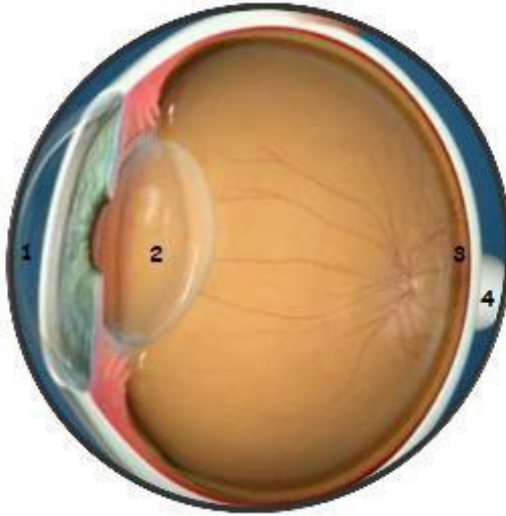


Figure 1: Structure of the human eye. Light passes through the cornea and the lens before being focused on the retina. Located in the anterior of the eye is the cornea (1), posterior to the cornea is the lens (2), which helps to further focus light onto the retina (3). Specialized cells called photoreceptors within the retina then relay the signal to the brain through the optic nerve (4), allowing us to see [43].

1.2 Structure of the lens

The lens is a relatively simple tissue that is composed of two distinct cell types, the epithelial and fiber cells [1]. The lens epithelium, located in single cell layer in the anterior of the lens, provides a source of precursor cells that differentiate into fiber cells, while also contributing to sustain the fiber cells metabolically [2] [1]. The central region of the lens is rendered clear because it is made of terminally differentiated fiber cells that are completely devoid of nuclei and organelles. The entire lens is enclosed by a thickened basement membrane termed the lens capsule, which provides structural integrity to the lens [1, 2]. The organelle-free central region is composed of the lens fiber cells, which provides the lens with its transparency.

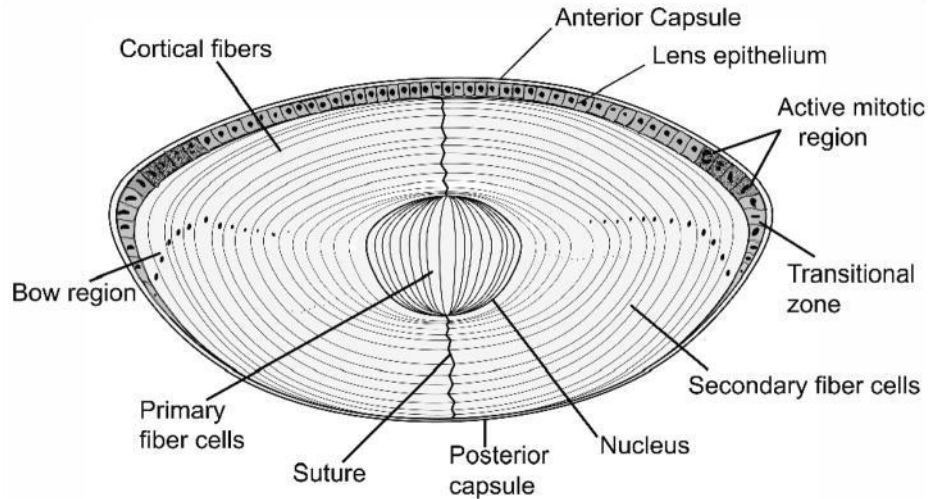


Figure 2: Structure of the mature lens. Cell division occurs in active mitotic regions of the anterior epithelium, and cells move laterally until they invert in the bow region of the lens. They then begin to differentiate into fiber cells that elongate, move toward the center of the cells where they meet with similarly migrated fiber cells but from the opposite end, and interact with them to form sutures [44]

1.3 Mammalian lens development

During embryonic development, at mouse embryonic day E9.5, the developing optic vesicle (that in later stages forms the retina) induces the overlying ectoderm to form a thickening termed the lens placode. The lens placode at stage E10.5 invaginates to first form a lens pit that pinches off from the surface ectoderm at E11.0 to develop into a hollow ball of epithelial cells (now termed the lens vesicle), which in turn will be surrounded by the lens capsule [45]. At mouse E11.5, the anterior part of the lens vesicle can already be classified into epithelial cells that begin to proliferate to form the cuboidal epithelium along the anterior surface, and the posterior part where epithelial cells stop proliferating, exit the cell cycle, and begin to elongate and differentiate into primary fiber cells [3]. As fiber cell differentiation proceeds further (stage

E14.5 and later), it is marked by the loss of organelles, including nuclei [4], which is necessary for the transparency and maximizing the refraction of light. Throughout the life of the organism, the epithelial cells located at the equatorial region of the lens continually divide and at the “transition zone” differentiate into new fiber cells. In this process, the new differentiating cells elongate and forms successive layers of fiber cells, which compact on the older fiber cells at the center of the lens [5]. Without this continuous process of differentiation and degradation of organelles, the clarity of the lens cannot be maintained.

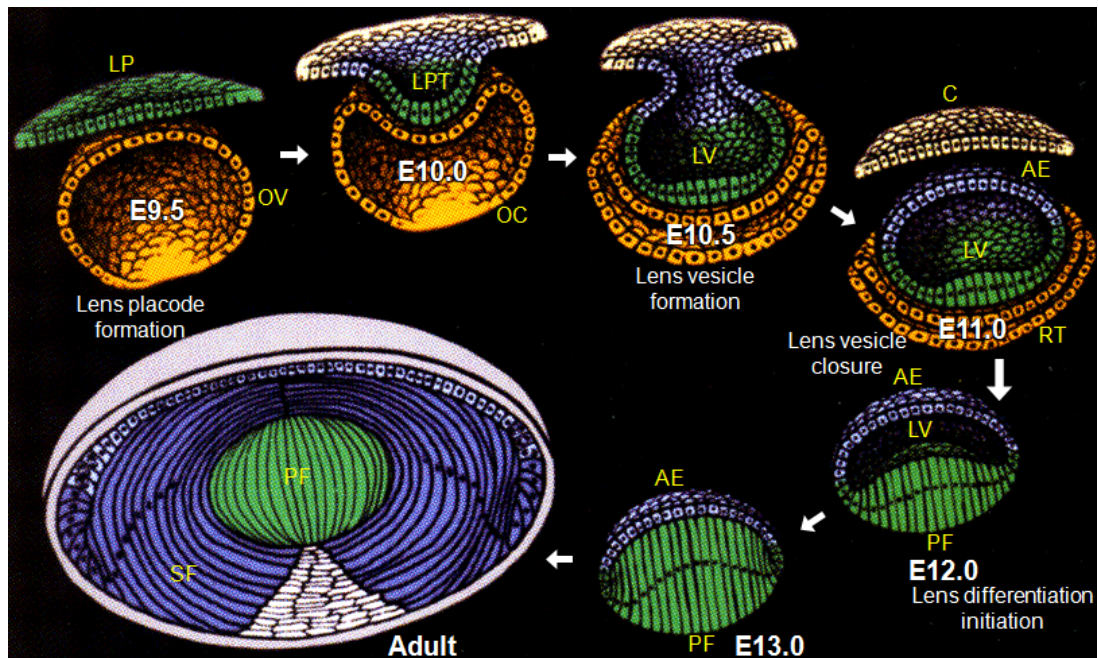


Figure 3: Lens development in mammals. In mouse, at embryonic day E9.5 the optic vesicle (OV) induces the surface ectoderm to form the lens placode (LP). The lens placode and the optic vesicle then develop coordinately to form the lens pit (LPT) and the optic cup (OC), respectively. At E10.5, the lens pit closes to form the lens vesicle (LV), which pinches off from the surface ectoderm that contributes to the formation of the cornea (C). At E11.5, epithelial cells located at the anterior part of the vesicle constitute the anterior epithelium (AE). At E11.5, epithelial cells that are located in the posterior part of the lens vesicle initiate differentiation into primary fiber (PF) cells that begin to elongate and fill up the lens vesicle. The lens vesicle is completely filled up by E13.0. Cells of the anterior epithelium differentiate into secondary fiber (SF) cells then elongate, differentiate and lose their organelles and pack tightly around the primary fiber cells. Differentiation of anterior epithelium cells into secondary fiber cells occurs throughout the life of the organism and is necessary to maintain lens transparency [46].

1.4 Cataracts: Definition and statistics

Genetic perturbations, physical or radiation based injury to the lens, or the natural process aging can lead to opacification or clouding of the lens, also known as cataract [45]. Based on the time of onset, cataracts can be either classified as congenital or age related [6, 7] [8]. Unlike the

most common form of cataracts, the age-related cataracts that occur in individuals aged 60 and above, congenital cataracts are present at birth. Depending upon population tested, around 25-50% of congenital cataracts are caused by genetic mutations.

The development of cataracts is not always genetically based. For example, physical trauma as a result of injury to the lens tissue can also cause cataract. Importantly, cataracts affect about 77 million individuals worldwide and its incidence is expected to increase globally with the rise in human life expectancy [9]. The only current treatment is cataract surgery, which often leads to a secondary cataract formation, an undesirable complication, especially in the elderly. Furthermore, underdeveloped countries have a higher number of individuals with impaired vision due to cataract compared to the developed countries, which may mostly reflect the difference in access to healthcare. In my thesis, I will be focusing on the study of a *Tdrd7* null mouse mutant model of childhood cataract to investigate the molecular changes that may contribute to this birth defect.



Figure 4: An example of how cataracts impair vision. The left image is an example of normal vision; the middle and right images are examples of progressively impaired vision as the clouding of the lens progresses [47].

1.5 Regulation of lens development

To begin to understand how misregulation of genes during development can lead to congenital cataracts, it is important to first discuss how lens development is normally regulated. Vertebrate eye development is initiated early in embryogenesis, during late gastrulation when the ectoderm is divided into four domains: neural plate, neural crest, preplacodal region (PPR), and anterior neural plate (ANP) that eventually form bilateral eyes. A single ‘presumptive retinal ectoderm’ (PRE) is formed in the region of the anterior neural plate (ANP) during late gastrulation at this stage [10-12](Figure 5).

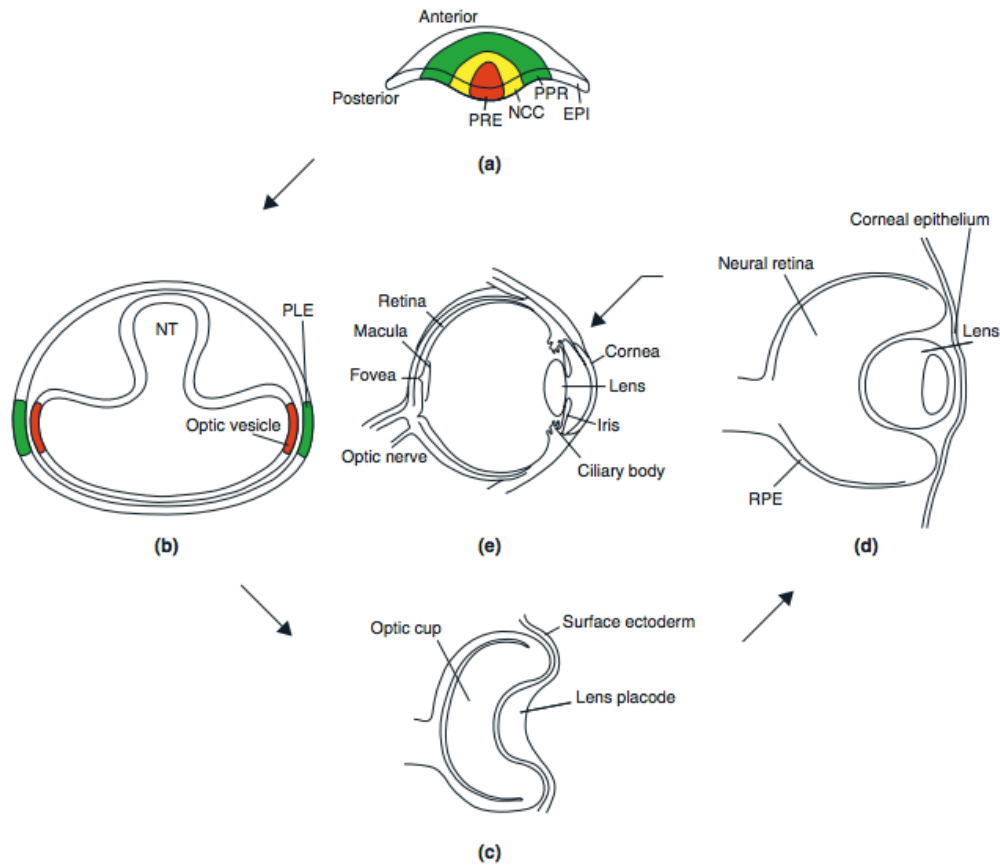


Figure 5: Vertebrate Ocular development. (a) The anterior neural plate contains the presumptive retinal ectoderm (PRE) (red) surrounded by the neural crest cells (NCCs) (yellow), preplacodal region (PPR) (green), and the epidermis (EPI) (white). (b) The closure of neural tube (NT), leads to the bilateral development of diencephalon into the optic vesicles, which comes in contact with the presumptive lens ectoderm (PLE) on either sides. (c) PLE forms into the lens placode by coordinate signaling; at the same time the optic vesicle invaginates to form the optic cup. (d) The lens placode invaginates and forms the lens pit that detaches from the surface ectoderm to form the lens vesicle. At this stage, the neural retina and retinal pigment epithelium (RPE) are formed by the initiation of optic vesicle invagination. (e) This shows that the adult vertebrate eye has multiple compartments.

As these distinct tissues are being formed, it is necessary to have accurate positioning of these tissues at the correct developmental space and time in order for proper development to occur. It is also important that there is a coordination of signaling molecules within and between these tissues. For example, the PPR can be identified by a combination of fibroblast growth

factors (FGF)-mediated positive regulators and the simultaneous inhibition of the negative regulators (the Bmp and Wnt signaling pathways) of this process. The correct signals that are required for the PPR to differentiate further are the transcription factors (TFs) Six3 and Foxg1 in mice. The fate of PRE is restricted by signaling molecules like Sonic hedgehog (Shh), Hes1, Lhx2, Otx2, Rx, Pax6, Sox2, and Six3 [13, 14]. One of the most critical TF expressed at this early time point is Pax6, without which the presumptive lens ectoderm (PLE) will fail to develop into the lens placode [15]. Bmp is a regulatory growth factor expressed in the PLE before lens placode induction begins during the regulation of lens development, [16, 17] [48]. Interestingly, Bmp7 loss-of-function embryos indicate a requirement for Bmp7 in maintaining Pax6 placodal expression. These developmental events, which are directed by a series of signaling molecules and TFs, lead to the invagination of the lens placode, transforming it into a lens pit, which develops into the lens vesicle.

As the cells located in the posterior region of the E11.5 lens vesicle differentiates into primary fiber cells (mentioned in 1.3) and degrade their cellular organelles, they must up-regulate an specialized lens proteins termed crystallins in order to maintain their cellular structure [18-20]. For example, *Cryaa*, which encodes Crystallin alpha A, is expressed in both lens epithelial region and in the lens fiber cells. Crystallin alpha B has been shown to inhibit apoptosis by slowing the maturation of caspase- 3, and is thought to be involved in preventing cell death in stressed cell [21].

Similarly, Crystallin Beta A1 in the lens maintains the transparency and refractive index of the lens. Since lens central fiber cells lose their nuclei during development, these crystallins are made and then retained throughout life, making them extremely stable proteins. Crystallin gamma A is one of the major protein components of the vertebrate eye lens. The regular

arrangement of the lens fiber cells during lens growth and the high concentration crystallin proteins allows for the high refractivity of light through the lens [49]

In mice at the E12.5 stage, differentiating fiber cells begin to down-regulate *Pax6*, whereas the ALE maintains its high expression. Importantly, *Pax6* also controls the expression of the Mab gene family member *Mab2111* that is required for lens placode development. Interestingly, *Mab2111* in turn regulates *Foxe3*, a highly lens-expressed TF gene that functions in regulating ALE proliferation, fiber cell differentiation, and lens vesicle closure [22-25]. In the ALE, *Foxe3* negatively regulates *Prox1*. Upon cell cycle exit, *Foxe3* is down regulated and the concurrent up regulation of *Prox1* in differentiating fiber cells is critical for their elongation and the expression of gamma crystallins.

1.6 *iSyTE* a tool for lens gene discovery

Genetic studies of inherited cataracts have identified mutations in about 25 genes that cause cataracts. However, genetic mapping is expensive and time consuming and biological insight is often helpful in the prioritization of candidate genes within mapped intervals. Therefore, Dr. Salil Lachke developed a bioinformatics-based tool called *iSyTE* (integrated Systems Tool for Eye gene discovery) [26]. *iSyTE* applies specially normalized mouse embryonic lens gene expression datasets to identify and prioritize candidate genes from human or mouse genomic regions implicated in eye disease. Using *iSyTE*, we can find previously identified as well as novel genes based on their high enrichment in the lens compared to the whole body reference dataset used in the normalization protocol. RNA further confirmed lens-enriched expression of candidate genes predicted by *iSyTE* *in situ* hybridization analysis [26]. *iSyTE* led to the

identification of *TDRD7* as a novel gene associated with cataract in human, mouse and chicken [27] [26].

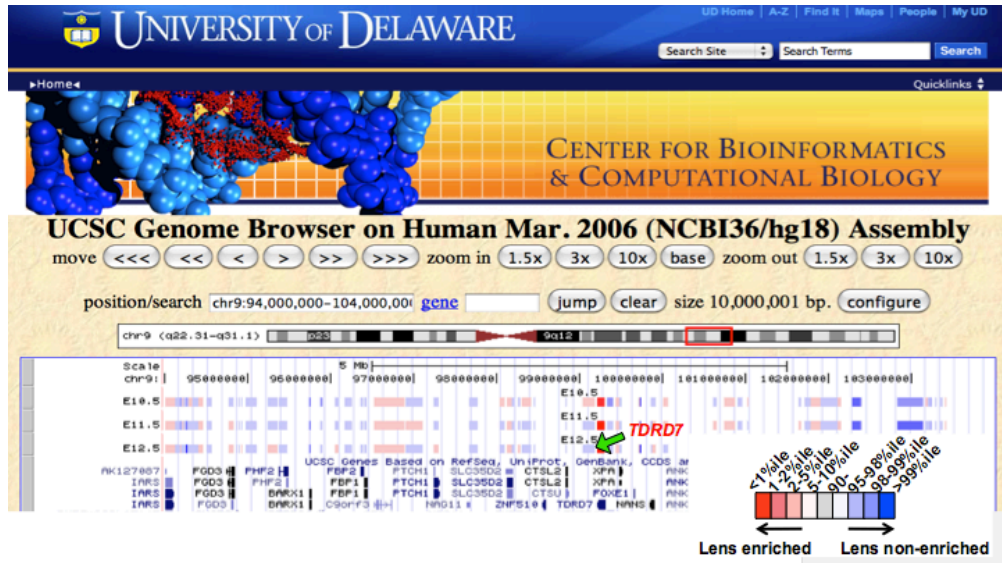


Figure 6: *iSyTE*: integrated Systems Tool for Eye gene discovery, uses mouse embryonic lens gene expression dataset as a bioinformatics filter to select candidate genes from human or mouse genomic regions implicated in disease and to prioritize them for further mutational and functional analyses [26].

1.7 *TDRD7*

Tdrd7 (Tudor domain containing 7) encodes a protein that contains three OST-HTH domains in its N terminus and three Tudor domains over the length of the protein (Figure 7). It is a putative RNA binding protein that is highly expressed in the lens fiber cells compared to the whole body control [27] and is considered to interact with RNA or methylated arginine residues within other proteins and may therefore act as a scaffold protein involved in sequestering proteins and RNA complexes. Majority of the known Tudor domain proteins are linked with RNA metabolism and control in the cell [28].

***TDRD7* (Tudor Domain Containing 7)**

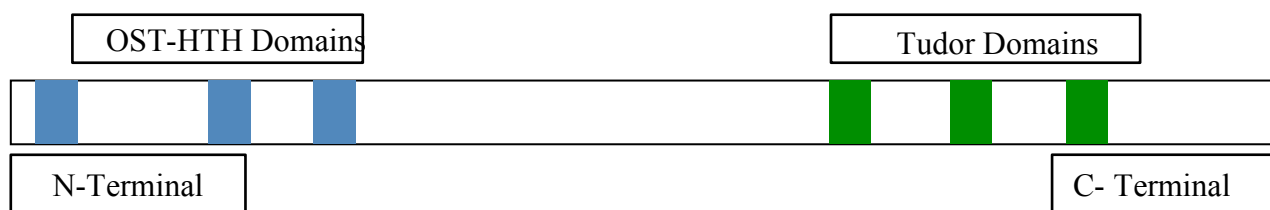


Figure 7: TDRD7 (Tudor domain containing 7). TDRD7 has three OST-HTH domains and three Tudor domains, predicted to interact with RNA and methylated arginine residues within other proteins, respectively.

1.8 Function of Tudor domain proteins in development and disease

Tudor domain proteins have been found to function as molecular adaptors. Tudor domains bind to methylated arginine or lysine residues on their substrates to promote physical interactions and function in assembling macromolecular complexes. Tudor domain proteins play a crucial role during development, and in other aspects such as RNA metabolism, the DNA damage response and chromatin modification [29]. Furthermore, deficiency in one of the Tudor domain proteins, Tdrd7 causes pediatric cataracts, glaucoma as well as male sterility defects (i.e., defective spermatogenesis) [26]. Therefore, Tudor domain proteins function in diverse cellular processes and have wide-ranging effects on developmental processes and cellular events [30]. Specifically, Tudor domain containing 7 (Tdrd7) is essential for dynamic ribonucleoprotein (RNP) remodeling of chromatid bodies during spermatogenesis [29].

1.9 *Tdrd7* deficiency and spermatogenesis defect

Sperms have specialized germinal granules, which are chromatid bodies that are composed of ribonucleoprotein (RNP) complexes. They are structurally detectable during early sperm development, meiosis and haploidgenesis, but their developmental origin and regulation are unknown [29]. The Tudor domain containing proteins constitute a conserved class of chromatid body components, deficiency of several causing male-specific sterility in mouse mutants. Mouse mutants null for *Tdrd7* exhibit sperms arrested in the post-meiotic round spermatid [29] stage and a complete absence of mature swimming sperms[29]. Interestingly, *Tdrd7* null mutant testes were found to be smaller than *Tdrd7* heterozygous testes at 10 weeks of age.

1.10 *Tdrd7* deficiency causes eye disease

Mutations in *TDRD7* have been associated with cataract formation in humans (Figure 8A) [27]. This was discovered when a male patient, designated DGAP186 as a part of the Developmental Genome Anatomy Project (DGAP) was found to have juvenile cataract and hypospadias caused by a *de novo* balanced paracentric inversion of chromosome 9,46,XY, inv(9)(q22.33q34.11) (Figure 8B). Analysis of 9q22.33 breakpoint showed that *TDRD7* was disrupted. The allelic disruption observed in DGAP186 lymphoblastoid cells results in *TDRD7* haploinsufficiency that is detected at both RNA and protein levels (Figure 8E). The potential mutant protein caused by this allelic defect is shown in the Figure 8B, although it should be noted that this smaller protein product was not detected in Western blotting. The independent involvement of *TDRD7* in pediatric cataract was confirmed by identifying a family, F3R (Figure 8E), with autosomal recessive congenital cataract. Using homozygous mapping, a single region

of shared homozygosity between four affected siblings that extended throughout the *TDRD7* locus was identified. Moreover, using bidirectional sequencing of *TDRD7*, a novel in-frame 3-base pair deletion that removes a highly conserved amino acid, V618 was identified (Figure 8F). This V618del variant, which was not detected in 320 ethnically matched controls (640 chromosomes), was predicted to disrupt the structure of *TDRD7* and was therefore likely to represent a loss-of-function mutation [27].

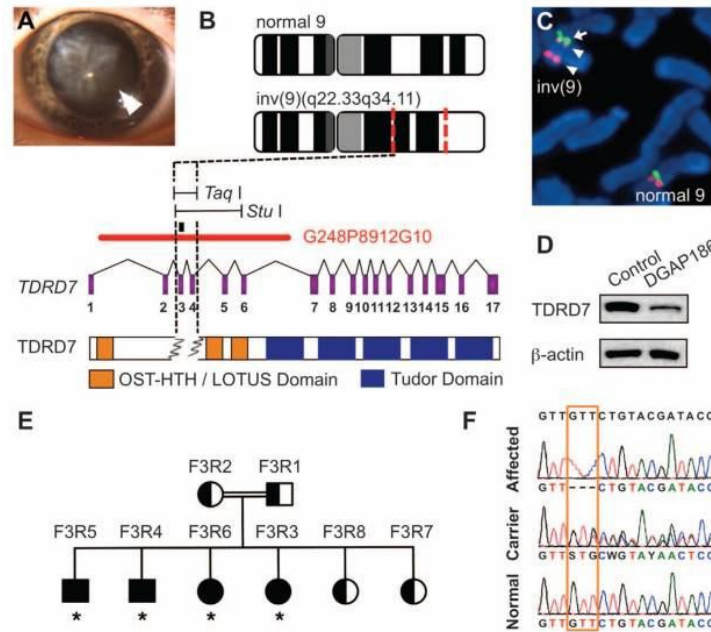


Figure 8: *TDRD7* mutations in human pediatric cataract. (A) Cataract in DGAP186 (left eye, white arrowhead). (B) Ideogram of normal and inverted chromosome 9 [inv(9)]. Red lines show inversion breakpoints, with a schematic below of the *TDRD7* gene and the resulting change in protein. Dotted black lines marks breakpoints that disrupt *TDRD7* within the 2.6-kb region shown and in *TDRD7* protein. The black bar indicates *TDRD7* genomic probe in Southern analysis. *TaqI* and *StuI* refer to the fragments resulting from restriction enzyme digest. The red bar indicates fosmid clone G248P8912G10 used as a *TDRD7*-specific probe. Purple boxes indicate exons. (C) Chromosomal spread of DGAP186 lymphoblastoid cells analyzed by fluorescence in situ hybridization shows split *TDRD7*-specific red probe, whereas green anchor probe remains intact in inv(9). (D) *TDRD7* haploinsufficiency is demonstrated by Western blot of DGAP186 lymphoblastoid cells. (E) Pedigree of consanguineous family F3R with congenital cataract (solid symbols, affected status; half-solid symbols, carrier status). (F) Sequence chromatogram shows c.1852_1854del (p.617delVal) mutation (boxed) in family F3R [27].

In *situ hybridization* of mouse and chicken embryos reveal strong and highly specific expression of *Tdrd7* transcripts in the developing mouse lens. *Tdrd7* is expressed in differentiating fiber cells in the posterior lens, whereas the expression is not measurable in the anterior epithelium (AEL) of the lens at embryonic day 12.5 (E12.5) [27]. In the chicken, retroviral injection into the E2 optic vesicle causes a cataract phenotype at E16 (Figure 9) at in complete penetrance. Mouse mutants with an N-ethyl-N-nitrosourea (ENU) - induced recessive

mutation in *Tdrd7* were identified during screening for ocular phenotypes. These mice developed severe cataracts (Figure 9) and exhibited high intraocular pressure (IOP). Within 4 weeks of birth, all *Tdrd7* homozygous mutants developed a posterior cataract that became more severe with age.

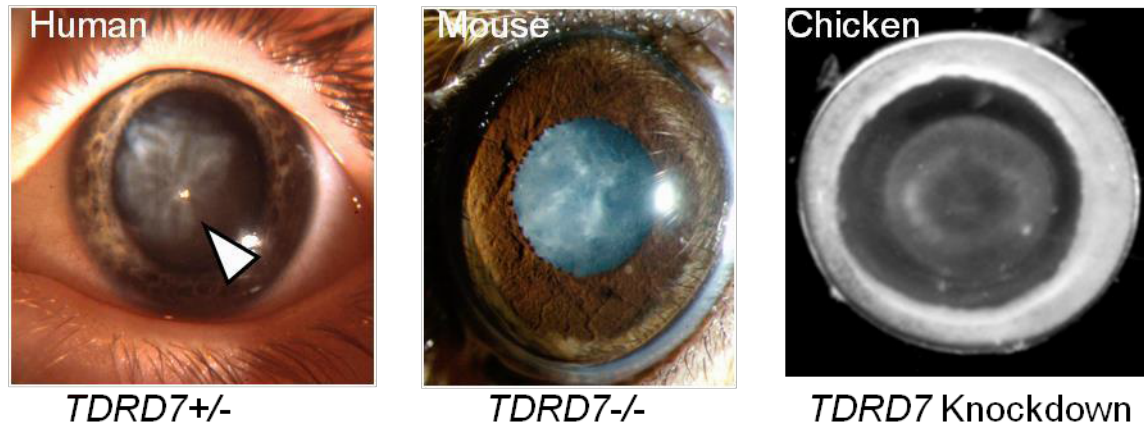


Figure 9: *TDRD7* Deficiency in human, mouse and chicken causes cataract [27].

At later stages lens fiber cells in *Tdrd7* null mutant lose connection with the surrounding tissue, exhibit capsular rupture, vacuole formation, and an exterior lens mass; all of which progressively worsens with age (Figure 10) [27].

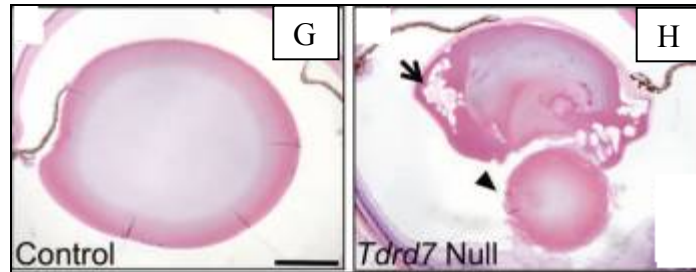


Figure 10: Lens defects in *Tdrd7* mouse mutant. (A) The histology of control lens at 3 months shows no ocular abnormality while (B) *Tdrd7* Null lens exhibit a severe cataract at the same age. Arrowhead points towards vacuole and the arrow indicates lens mass and the arrow shows capsule rupture.

1.11 *Tdrd7* lens specific RNA granules (RG)

As mentioned, Tudor domain proteins function in diverse cellular processes and TDRD7 has been found to be essential for dynamic ribonucleoproteins (RNPs) remodeling of chromatid bodies during spermatogenesis, which are differentially associated with one of the types of lens cytoplasmic RNA granules (RGs), known as the Processing Bodies (PBs). PBs are constitutively found in all cells, but can also be stimulated to form by stress, and are often found in association with components involved in microRNA mediated silencing, nonsense-mediated decay (NMD), and with enzymes involved in mRNA decay process [31]. Recently it was also found that TDRD7 is a RNA granule component that is highly enriched in the developing lens and shows an evolutionarily conserved pattern of expression. RNA granules (RGs) are found in the cytoplasm of eukaryotic cells from yeast to vertebrates. They are ribonucleoproteins complexes that are involved in the regulation of various aspects of mRNA control. Their function may include mRNA localization within cells and its stabilization or degradation [32-34]. Additionally, RGs include several proteins that are likely to function in development, but their full significance in this process, particularly in vertebrates, is not well understood [35]. Along with PBs, TDRD7 is

also associated with other cytoplasmic RNPs that contain a well-characterized RG component, Staufen1 ribonucleoproteins (Stau1 RNPs).

1.12 Regional co-localization with Stau1

Staufen1 (STAU1) is a double stranded RNA binding protein [36-38] that has a conserved function in RNA transport. Its function is conserved in animals as different as *Drosophila* and human and in cell types as distinct as oocytes and neurons [36]. In addition, STAU1 plays an important role in STAU1-mediated mRNA decay (SMD) by directly binding to mRNA their 3'-untranslated regions (3' UTRs) by active translation, and channeling them for degradation [39]. Interestingly, STAU1 has been found to highly colocalize with TDRD7 in lens fiber cells [27]. This colocalization between STAU1 and TDRD7 can be observed as early as E10.5 in the lens, and at stage E11.5, the expression is highest along the anterior edge of the elongating fiber cells (Figure 11). Since STAU1 is involved in RNA transport and it also colocalizes with TDRD7, it led me to my hypothesis that specific RNAs are localized in mouse lens fiber cells and TDRD7 is involved in actively transporting RNA in the elongated fiber cells. Therefore, I sought to determine if there are differences in mRNA localization between the apical and basal regions of the developing fiber cells at E12.5 and if these change in *Tdrd7* mutant lens.

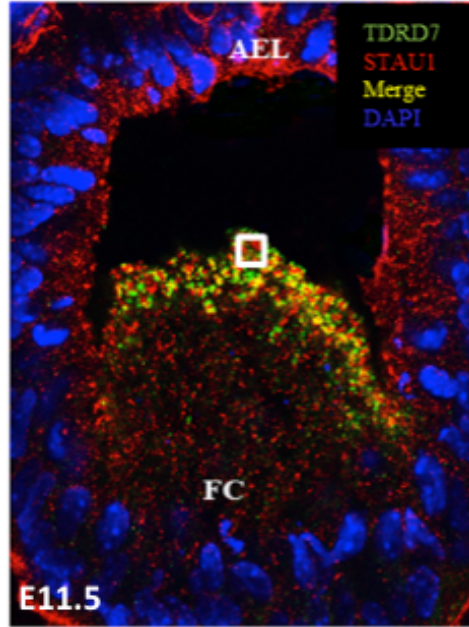


Figure 11: At E11.5, TDRD7 and STAUI expression shows a high degree of co-localization (yellow) in the anterior portion of the FC compartment. DAPI-stained nuclei are blue. (Inset) Higher magnification demonstrates high degree of colocalization (yellow) of TDRD7-RGs and STAUI-RNPs [27].

To test this hypothesis I will first identify preferentially localized candidate lens mRNAs in the apical and basal regions of *Tdrd7*^{+/-} (control) fiber cells using Laser Capture Microdissection (LCM). Followed by that, my second aim will be to test the misregulation of select candidate genes in the apical and basal fiber cell regions of *Tdrd7* null mutant mice using reverse transcriptase combined with polymerase chain reaction (RT-PCR) analysis.

Chapter 2

Methods and Materials

2.1 Animals

The University of Delaware Institute of Animal Care and Use committee approved all experiments using animals. All animals were treated in accordance with the protocols established by the Association for Research in Vision and Ophthalmology (ARVO). C57/B16 *Tdrd7* heterozygous mice were a kind gift from Dr. Shinichiro Chuma from Japan. *Tdrd7* homozygous mutant mice were generated by deleting exons 8-12 of the *Tdrd7* gene. Mice used in this project were produced at the University of Delaware OLAM facility in a specific pathogen free environment with a 14/10-hour light/dark cycle. Embryos used in the study were staged by designating the day on which the vaginal plug was observed as embryonic day (E)0.5 and allowed to gestate to E12.5. Postnatal mice were staged by designating the day of birth as P0.

2.2 DNA Isolation from Mouse Tails

Approximately 1-cm long tail samples were obtained from the mice in a 1.5-mL eppendorf tube and stored at -20°C until needed for genotyping. The Puregene® Genomic DNA Purification Kit (Gentra Systems, Minneapolis, Minnesota) was used to isolate genomic DNA. PCR amplification was performed on a BioRad® T100 Thermal Cycler (Hercules, CA). Three-hundred microliter of Cell Lysis solution and 1.5 µl of 10 mg/ml Protein K Solution were added

to the tail sample for tissue digestion and cell lysis. The samples were mixed by inverting 25 times and incubated at 55°C overnight with shaking. One-hundred microliter of Protein Precipitate solution was added, the samples were inverted times and centrifuged at 13,000 g for three minutes to form a precipitated protein pellet. If a pellet did not form, the samples were inverted again followed by incubation on ice for 15 minutes and centrifuged again. The supernatant containing the DNA was transferred to a clean 1.5-mL Eppendorf tube containing 300 µl of 100% isopropanol. The sample was mixed by inverting 25-30 times and pelleted by centrifugation at 13,000 g for six minutes. The supernatant was removed carefully, leaving the pellet intact. The pellet was washed by adding 300 µl of 70% ethanol (EtOH) and inverted 25 times to wash the DNA pellet, followed by centrifugation at 13,000 g for seven minutes. The ethanol was carefully removed via pipette and the samples were allowed to air dry for 30-35 minutes at room temperature (RT). The DNA pellet was rehydrated with 45-100 µl of DNA hydration solution, followed by incubation at 65°C for 1 hour. The incubated samples were mixed overnight on a shaker at 100 rpm at room temperature (RT). Once the DNA was isolated, the samples were quantified with a NanoDrop® ND 1000 Spectrophotometer (NanoDrop, Wilmington, Delaware) and stored at room temperature (RT) until needed.

2.3 Mouse Genotyping by PCR

Polymerase Chain Reaction (PCR) was done for each sample by adding 72.5% (18.125 µl) of ultrapure distilled water, 2.5% (0.5 µl) of each forward and reverse primer, 2.5% (0.5 µl) dNTP, 10% (2.5 µl) of CoralLoad PCR Buffer (Qiagen), Valencia, California), 5% (1.25 µl) dimethyl sulfoxide (DMSO), Fisher BioReagents™ (Thermo Fisher Scientific, Waltham, Massachusetts), 2.5% (0.5 µl) Taq DNA polymerase and 4% (1 µl) of genomic DNA into a 1.5-

mL microcentrifuge tube. The samples were mixed 25X and spun down. The spun microcentrifuge tubes were placed into the BioRad® T100 al Cyclor PCR machine. The TDRD7 cycling program was used (95°C for 2 minutes, 40 cycles at 95°C for 20 seconds, 55°C for 30 seconds, 68°C for 1 minute. After completion of the cycles, the samples were held at 4°C).

2.4 Agarose Gel Electrophoresis

Amplified DNA was size separated on a 1% agarose gel, made by dissolving agarose (Agarose LE-Molecular Biology Grade) in 1X TBE (Tris- borate- EDTA). To prepare the 1% agarose gel with 20 wells, 1.1 g of high melting agarose powder was dissolved in 100 ml of 1X TBE buffer. Ethidium Bromide (EtBr) (10 µL of a 0.01% solution) (Thermo Fischer Scientific, Waltham, Massachusetts) was added to the 1% agarose gel before it solidified to be able to visualize the DNA. The samples were size separated using approximately 95 volts for 60 minutes. A 1000-bp DNA ladder was used to determine the band sizes of the DNA fragments for heterozygous (control) and mutant bands (Thermo Fischer Scientific, Waltham, Massachusetts). Agarose gels were imaged using the GelDoc-IT® 2 310 imager (UVP Upland, CA). The band sizes were determined both for heterozygous (Het) (195 bp) and knockout (KO) (500 bp).

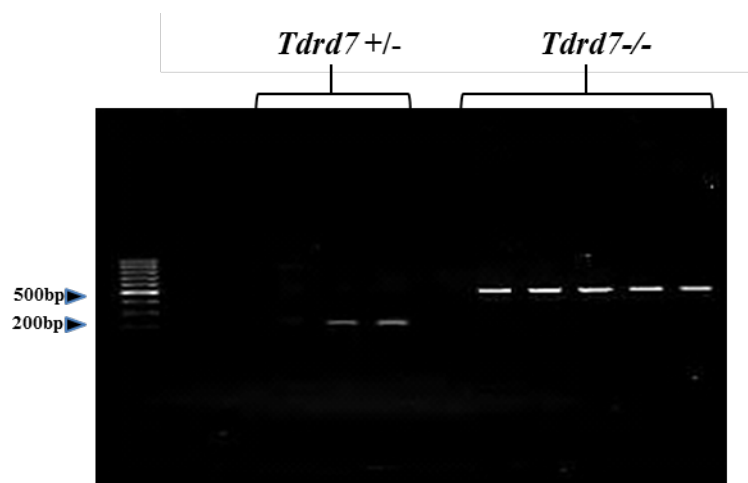


Figure 12: The band sizes were determined both for Het (195bp, lower band in the gel) and KO (500bp, upper band in the gel) DNA samples, respectively.

2.5 Isolation of Embryos

Female *Tdrd7*^{-/-} mice were mated with *Tdrd7*^{+/-} males and observed for a vaginal plug between 7-8 am which was considered day 0.5 Post Coitum (dpc). For E12.5 samples, pregnant mice were euthanized according to IACUC; 5 – 7 minutes exposure to CO₂ administered at 3 pounds per square inch (psi). An incision was made along the ventral midline from the vagina to the ribcage, opening the body cavity. Incisions were then made perpendicular to the initial incision on either side of the lower abdomen to open up the body cavity further. The embryos were removed along with the uterus and placed in a petri dish filled with 1X PBS. The embryos were removed from the uterus followed by removal from the embryonic sac in a petri dish with 1x PBS. For sectioning purposes, the heads were separated from the body with forceps and placed in 1X PBS, followed by a 1:1 equal mixture of 1X PBS and O.C.T, and finally 100% O.C.T for 10-15 seconds each. Once the embryonic head was saturated in O.C.T, it was

embedded nose down in a Tissue-Tek(R) Cryomold(R) (Sakura(R) Finetek, Torrance, California) filled with O.C.T. Compound and immediately placed at -80°C, or on dry ice, to freeze and store the samples.

2.6 Cryostat

The cryostat was set at -22°C for Outer Temperature (OC) and -26°C Cutting Temperature (CT), respectively. Prior to use, the cryostat was cleaned with 90% EtOH and the tissue and tools needed were placed in the cryostat chamber to bring it to the chamber temperature. The specialized LCM slides were left at room temperature in order to make it easier for the samples to stick to the film of the slide. The sample pedestal was placed inside the cryostat for 10 minutes and allowed to reach the chamber temperature. O.C.T. was added to the pedestal and the sample was mounted on the O.C.T. with the back of the embryonic head towards the pedestal (nose facing out) and placed in the chamber for 5 minutes to solidify. Once the O.C.T. began to freeze, an additional mount was added to the side of the block to make the mount stronger and secure it to the base. The lever on the right was released to adjust the plane of the specimen. The adjustments were made in a way that the angle between the plane and the moving pulley was 0° and the section thickness was set to 14 µm. The pedestal was put to the head home position and the blade secured in the mount. The sections were collected on specialized Laser Capture Microdissection (LCM) slides (catalog#1475434). The slides were allowed to air dry for about 2 minutes and stored at -80°C.

2.7 Laser Capture Microdissection (LCM)

LCM was carried out using The Zeiss Laser Microdissection (P.A.L.M) CombiSystem from Carl Zeiss (Germany), which utilizes Laser Pressure Catapulting (LPC) technology for isolating individual cut cells (Figure 13). A membranous slide was placed membrane side up. Apical/basal fiber cell pools (all the fiber cells from the apical/basal regions, respectively) were collected on different sides. The apical/basal lateral fiber cell tissue was visualized in ‘transmitted light’ mode on the PalmRobo software was used for cutting the sample with a pulsed Nitrogen UV laser (337 nm wavelength) along the perimeter of the defined square. Care was taken to direct the laser at the edge of the apical and basal lateral areas of the E12.5 lens, adjacent to the selected area, therefore only the region at the edge of the fiber cells was taken. The dissection conditions were optimized to obtain a clean, narrow excision of the selected area: 20x objective at power 65 to 85 and speed 20 to 22. Once the laser had cut the selected area, the specimen was catapulted into a PALM® adhesive cap (Cat # 1440-0250, P.A.L.M. Micro Laser Technologies AG, Germany). First the apical region was captured followed by the basal lateral region. To avoid degradation of cellular mRNAs, capture was limited to 45 minutes. On average 3-4 apical and basal lateral regions were captured per heterozygous and null slides. In total 88 and 66 fiber cell pools were taken from 20/22 slides to extract the RNA for reverse transcriptase-PCR (RT-PCR).

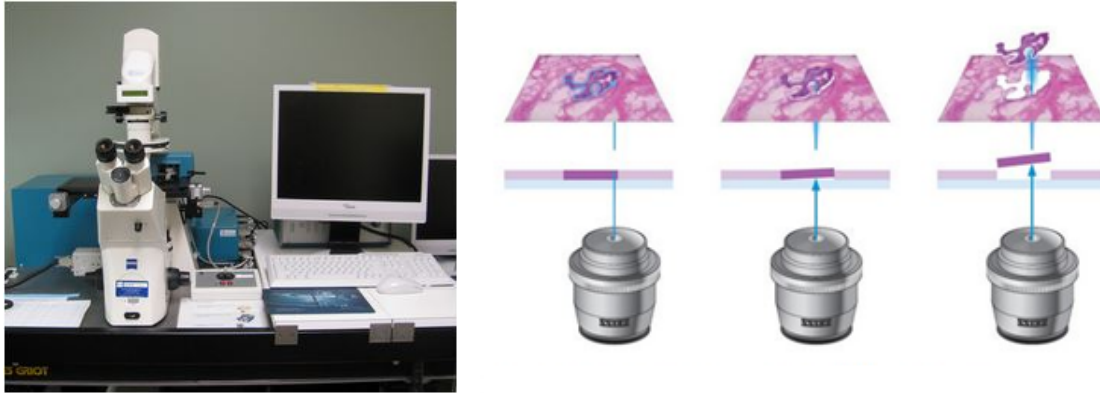


Figure 13: Laser Capture Microdissection (LCM) microscope and technology. (A) The inverted P.A.L.M. Laser Capture Microdissection. (B) Schematic of selected regions defocuses and catapults the sample into the 0.5-ml P.A.L.M. adhesive cap held above by a robo mover. (DBI, University of Gothenburg, CCI).

2.8 RNA isolation

The PicoPure™ RNA Isolation Kit (Life Technologies) enabled us to recover the total RNA from Pico-scale tissue that was acquired using Laser Capture Microdissection (LCM) Caps. Prior to starting the protocol, the lab bench, pipettes and pestles were cleaned with 70% EtOH and RNase Away, (Catalog #50212367, Fischer Scientific) to prevent any foreign nucleic acid contamination. Ten microliter of Extraction Buffer (XB) was pipetted onto the topside of the LCM microcentrifuge tube and the cap was closed tightly to avoid any contact with the atmosphere. The microcentrifuge was inverted and tapped to ensure all the XB was covering the sample. The tube was incubated inverted for 30 minutes at 42°C and centrifuged at 800 x g for 2 minutes. The samples from 20/22 caps at a time (total of 88 caps) were combined and 10 µl of 70% EtOH was added for each cap. Once the tissue material was dissolved and on the bottom of the tube, the samples could be stored at -80°C if needed. To precondition the RNA Purification column, 250 µl Conditioning Buffer was pipetted onto the purification column filter membrane.

The RNA Purification Column was incubated with the Conditioning Buffer for five minutes at RT. The column was centrifuged for one minute at 16,000-x g to remove the conditioning buffer. To each sample, the same amount (10 µl) of molecular grade 70% EtOH was added. This mixture was mixed gently using a pipette. The tissue extract was added to the preconditioned purification column. The mixture was centrifuged for two minutes at 100-x g immediately followed by centrifugation at 16,000-x g for 30 seconds. The Flow through was removed.

For DNase treatment, 100 µl of Wash Buffer 1 (W1) was pipetted into the purification column and centrifuged for one minute at 8,000-x g. Five µl of DNase I stock Solution of 35 µl of Buffer RDD was pipetted and mixed gently by inverting. Forty µl of DNase incubation mix was pipetted directly onto the purification column membrane and was incubated at room temperature (RT) for 15 minutes. Another 40 µl of PicoPure RNA kit Buffer 1 (W1) was pipetted onto the column membrane and centrifuged at 8,000 g for 15 seconds. Wash Buffer 2 (W2) was pipetted into the purification column and centrifuged for one minute at 8000-x g. An additional 100 µl of W2 was pipetted into the purification column and centrifuged for two minutes at 16,000-x g. If the buffer remained, it was re-centrifuged at 16,000-x g for one minute. The purification column was transferred to a new 0.5-µl-microcentrifuge tube. Eleven µl of Elution Buffer (EB) was pipetted directly onto the surface of the membrane and dispersed to ensure maximum absorption of EB into the membrane. The purification column was incubated for one minute at RT. Finally; the column was centrifuged for one minute at 1,000-x g to distribute the EB in the column followed by centrifugation at 16,000-x g to elute the RNA. The RNA was tested on a Nanodrop for quantity and purity, and stored at -80°C.

2.9 cDNA synthesis for Reverse Transcriptase-PCR

Reverse transcriptase (RT) PCR was performed in two steps, cDNA synthesis and PCR. Total RNA concentration was measured using a NanoDrop® ND 1000 Spectrophotometer (NanoDrop, Wilmington, Delaware) and the amounts of RNA were calculated. Master Mix was prepared for iScript Reaction Mix and nuclease-free water was added in a way to make the final volume 20 µl, depending on the amount of RNA template (1 µg of total RNA). The master mix was combined in one tube and 4 µl of 5x Reaction Buffer was added followed by 1 µl of reverse transcriptase per reaction. The samples were briefly vortexed and spun down. BIO-RAD Thermal Cycler was used for the cDNA synthesis. The samples were treated at 25°C for 5 minute, 42°C for 30 minutes, 85°C for 5 minutes and infinitely held at 4°C. After the process was done, tubes were taken out and stored at -20°C until needed for RT-PCR.

2.10 Reverse Transcriptase-PCR (RT-PCR)

cDNA was diluted to 100ng/µl and a Polymerase Chain Reaction (RT-PCR) was performed to validate gene expression in the apical and basal fiber cell samples. RT-PCR was carried out by adding 19.625 µl of water, 2.5 µl Coral Red Buffer (10X), 0.5 of 100 µM forward and reverse primers, 0.5 µl of the cDNA, and 0.125 µl of Taq Polymerase.

2.11 Primer design

Gene option under NCBI was selected and the gene name was typed in and *Mus Musculus* was selected. The longest isoform under mRNA and Proteins was picked and FASTA was

selected. The isoform was copied and pasted into the web-based primer design program Primer 3 (<http://bioinfo.ut.ee/primer3/>) and product range was set 150-300bp. forward and reverse primers were chosen and primer quality was checked using Sequence Manipulation Suite (SMS). Parameters like self-annealing and hairpin formation was confirmed to be “pass”= good.

Table 1: Primers used for amplification of reverse-transcribed mRNAs originating from genes of interest.

Gene	Forward Primer Sequence	Reverse Primer Sequence	Expected Product Size (In basepairs)
<i>ActB</i>	TGTTACCAACTGGGACGACA	GGGGTGTGAAGGTCTCAA	228
<i>Cryaa</i>	GACCCTGTGCTCTCCTCAAG	AGCATGTGGTTGGTGCATTA	211
	GCCGTGGTAGCTGAAGAGAC	GCCAGCTAAGATGCACATGA	160
<i>Cryab</i>	TGGGCTAGGAACATTTGGAG	CAGTTACAATTCGGGGCACT	169
	GCCGTGAGCTGGGATAATAA	CGAAGAACTGGTTCGAAGAGG	219
<i>Crybal</i>	GGAAACTCTTCCAACCACCA	CCACTGGCGTCCAATAAAGT	228
	CTTTGAGCAATCTGCCTTCC	GTGCCACCAGAGACGGTTAT	180
<i>Crybb1</i>	GGAGCTACAGGCTGATCGTC	GTGCCACCAGAGACGGTTAT	267
<i>Cryga</i>	GCCGTTCCATTCCATACACCA	CTGTAACAAGCAAAGGAGG	311
<i>Crygd</i>	ACCCTGACTACCAGCAGTGG	GTCGTGGTAGCGCCTGTACT	281
<i>E-Cadherin</i>	CACACCCTGACCAAAGTCCT	AGGGGTGTCTGTGAAAGGTG	252
	AGTTTACCCAGCCGGTCTTT	AAGAGCAGGTCGGAACCTCA	155
<i>Foxe3</i>	GAAGCCGCCCTACTCATACA	AGGAAGCTACCGTTGTCGAA	273
<i>Gapdh</i>	CCGCATCTTCTTGTGCAGT	GAATTTGCCCGTGAGTGGAGT	204
<i>GPR151</i>	TTCGTCTTCAGCCTGACCTT	CGGTTCCCTGTGATCTTCAT	236
	TCATCGGTGGAGTTTGATGA	TGATGAGAAAGGGGAACAGG	112
<i>Htra3</i>	CCGTCGTGCGTTGCAGGTCT	GTTTCCCCATCCTTTTCGTT	461

<i>Mupc</i>	CCTGGCCTCTGACAAAAGAG	AACGAAAAGGATGGGGAAAC	214
	TGCCGATGGCCACCACGAAC	CACTCAACACTGGAGGCTCA	165
<i>Pax6</i>	AGTTCTTCGCAACCTGGCTA	ACTTGGACGGGAACTGACAC	846
<i>Prox1</i>	CTGGGCCAATTATCACCAGT	GCCATCTTCAAAGCTCGTC	205
<i>Tdrd7</i>	CTAAGGGCTGTCCTGCAGTC	TGAGAGTTGCCTTTGGCTTT	340
<i>Trpm3</i>	GGGTCGCCAGGCAAGCCATT	CCGGCAGCACACATGCTGGA	461

Table 2: Genes and their function in the lens

Gene	Type of marker	Function in the lens
<i>Foxe3</i>	Lens epithelial marker	Essential for lens epithelial proliferation and closure of the lens vesicle.
<i>Gapdh</i>	Housekeeping marker	Expressed at relatively constant levels in most non-pathological situations in the lens fiber cells
<i>Cryaa</i>	Both fiber cell and epithelial marker	Expressed in both lens epithelial and fiber cells
<i>Cryab</i>	Both fiber cell and epithelial marker	α B has been shown to inhibit apoptosis by slowing the maturation of caspase-3, and may be involved in preventing cell death in stressed cells [21].
<i>Cryb1</i>	Both fiber cell and epithelial marker	Lens and maintains the transparency and refractive index of the lens. Since lens central fiber cells lose their nuclei during development, these crystallins are made and then retained throughout life, making them extremely stable proteins.
<i>Cryga</i>	Both fiber cell and epithelial marker	Necessary for focusing visible light on the retina is achieved by a regular arrangement of the lens fiber cells during growth of the lenticular body and by the high concentration and the supramolecular organization, and gamma-crystallins, the major protein components of the vertebrate eye lens (summary by Moormann et al., 1982).
<i>E-cadherin</i>	Lens	Essential for normal cell sorting and subsequent

	epithelial marker	lens vesicle separation [40]
<i>Hprt</i>	Housekeeping gene marker	HPRT knockdown causes a marked switch from neuronal to glial gene expression and dysregulates expression of Sox2 and its regulator
<i>Hspb1</i>	Heat shock protein	Helps protect cells under adverse conditions such as infection, inflammation, exposure to toxins, elevated temperature, injury, and disease (genetics home reference)
<i>Htra3</i>	Lens anterior (epithelial) marker.	Expressed in the anterior surface of lens, but not expressed in the lens fibers (Jiraporn Tocharus, PhD. Thesis, Japan)
<i>Pax6</i>	Lens fiber cell marker	Essential for lens fiber cell differentiation [41]
<i>Prox1</i>	Lens fiber cell marker	Crucial for terminal fiber differentiation and elongation [23]
<i>Trpm3</i>	Lens fiber cell marker	Important for cellular calcium signaling and homeostasis. The protein encoded by this gene mediates calcium entry, and this entry is potentiated by calcium store depletion. Alternatively spliced transcript variants encoding different isoforms have been identified.
<i>Tdrd7</i>	Lens fiber cell marker	Component of specific cytoplasmic RNA granules involved in post-transcriptional regulation of specific genes: probably acts by binding to specific mRNAs and regulating their translation. Required for lens during lens development, by regulating translation of genes such as CRYBB3 and HSPB1 in the developing lens. Also required during spermatogenesis transparency

Chapter 3

Results

3.1 Laser Capture Microdissection

To test my hypothesis that mRNA may be localized in distinct regions in lens fiber cells and that TDRD7 may be involved in this process, I used Laser Capture Microdissection (LCM) as an approach to collect the apical and basal fiber cell regions from sectioned lens tissue from *Tdrd7*^{-/-} and *Tdrd7*^{+/-} mice (Table 3, Figure 13). As shown in Figure 13, the apical and the basal regions of lens fiber cells were selected using a tool called the PalmRobo. A laser was used to cut the tissue of interest, which was pushed into an eppendorf and stored at -80°C for RNA isolation experiment.

As shown in Table 3, a total of 294 LCM dissections of the apical and basal fiber cell regions were collected over a time interval of approximately 3 months (Table 3). For the heterozygous apical region, a total of 88 samples were collected in 22 eppendorf tubes. Similarly, 60 apical mutant samples in 20 eppendorfs, 80 heterozygous basal samples in 20 eppendorfs, and 66 mutant basal samples each were collected in 22 eppendorfs.

Table 3: Total number of samples collected by LCM from the apical and basal lens fiber cell regions from *Tdrd7*^{-/-} and *Tdrd7*^{+/-} mouse lens tissue.

Region of the lens	Number of eppendorfs	Number of samples in each eppendorf	Total Number of samples
Apical <i>Tdrd7</i> ^{+/-}	22	4	88
Apical <i>Tdrd7</i> ^{-/-}	20	3	60
Basal <i>Tdrd7</i> ^{+/-}	20	4	80
Basal <i>Tdrd7</i> ^{-/-}	22	3	66

3.2 RNA isolation from LCM captured tissue

Samples obtained from LCM were stored at -80°C for RNA isolation purposes. Once all the samples were collected, the eppendorfs containing the tissue were processed for an in-house RNA isolation.

Two biological replicates from each tissue type were prepared according to process explained in Materials and Methods and their concentrations were determined using the NanoDrop® ND 1000 Spectrophotometer. The RNA quantity obtained is shown in Table 4. Briefly, concentration of apical heterozygous replicate 1 was 14 ng/μl and replicate 2 was 5.3 ng/μl; concentration of apical null replicate 1 was 17.6 ng/μl, and that of replicate 2 was 12.9 ng/μl. The same experiment was performed on the basal region of the lens fiber samples. The RNA concentrations of basal heterozygous replicate 1, replicate 2, basal null replicate1, and replicate 2 were 1.7 ng/μl, 7.5 ng/μl, 17.5 ng/μl, and 2.5 ng/μl respectively.

Table 4: RNA concentrations of samples from different regions of the fiber cells.

Sample	Number of tissue samples per replicate	RNA concentration obtained
Apical <i>Tdrd7</i> ^{+/-} #1	22	14 ng/ μ l
Apical <i>Tdrd7</i> ^{+/-} #2	22	5.3 ng/ μ l
Apical <i>Tdrd7</i> ^{-/-} #1	30	17.6 ng/ μ l
Apical <i>Tdrd7</i> ^{-/-} #2	30	12.9 ng/ μ l
Basal <i>Tdrd7</i> ^{+/-} #1	40	1.7 ng/ μ l
Basal <i>Tdrd7</i> ^{+/-} #2	40	7.5 ng/ μ l
Basal <i>Tdrd7</i> ^{-/-} #1	22	17.5 ng/ μ l
Basal <i>Tdrd7</i> ^{-/-} #2	22	2.5 ng/ μ l

3.3 RT-PCR on LCM captured lens tissue

Next, I sought to test whether the LCM samples collected from the developing lens fiber cells were in sufficient quantities to produce cDNA that could be used in RT-PCR analysis. I designed primers specific for select lens markers as shown in Table 1 that were used in RT-PCR. Primers were designed for both epithelial and fiber cell marker genes. Using RT-PCR, it was shown that E-cadherin, a marker for lens epithelial cells, was not expressed in the lens apical or basal fiber cell regions (Figure 14). *Prox1*, a lens fiber cell marker, was expressed at similar levels in the *Tdrd7* heterozygous (control) and null (test) apical regions of lens fiber cells. Interestingly, *Prox1* expression was distinctly lower in the *Tdrd7* null basal fiber cells as

compared to *Tdrd7*^{+/-} controls. *Foxe3*, another marker for lens epithelial cells, was shown to express equally in all the apical and basal regions of the lens fiber cells. A housekeeping marker, *Gapdh*, was used which was expressed at similar levels in the apical and basal regions of the lens fiber cells.

I also tested the expression of crystallin encoding genes *Cryaa*, *Cryab*, *Cryba1*, *Crybb1*, and *Cryga* in the LCM captured apical and basal tissue (Figure 15). I found that *Cryaa* was expressed more in the apical region compared to the basal region of the *Tdrd7* heterozygous mice in the lens fiber cells. However, *Cryab*, *Cryba1*, *Crybb1*, and *Cryga* were expressed at similar levels in both apical and basal region of the lens fiber cells of *Tdrd7* heterozygous mice.

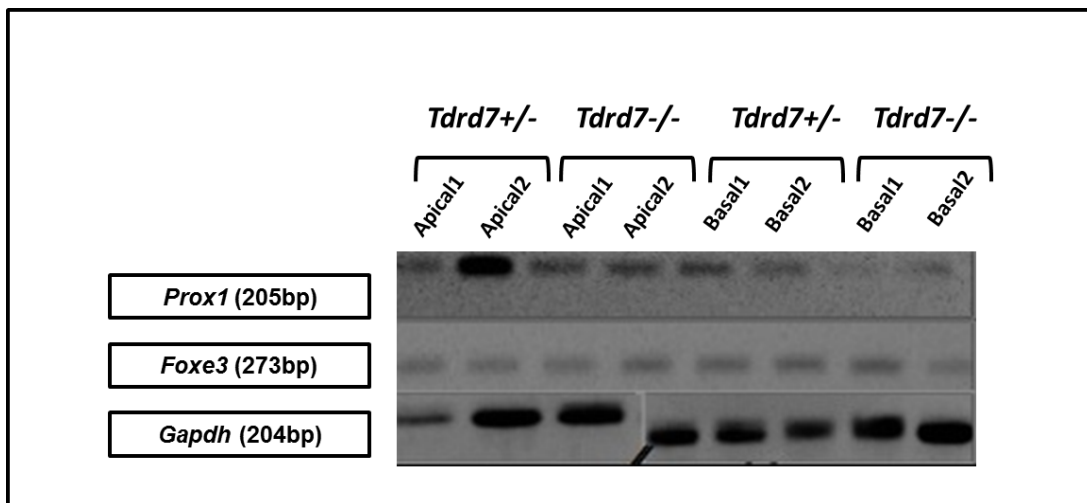


Figure 14: RT-PCR analysis of LCM captured apical and basal lens tissue. RT-PCR analysis exhibits that *Gapdh*, housekeeping marker, and *Foxe3*, a lens epithelial marker, were expressed equally throughout the apical and basal fiber cells for both *Tdrd7* null and control lens tissue. However, the expression of *Prox1* was considerably low in the *Tdrd7* null basal fiber cells in the lens.

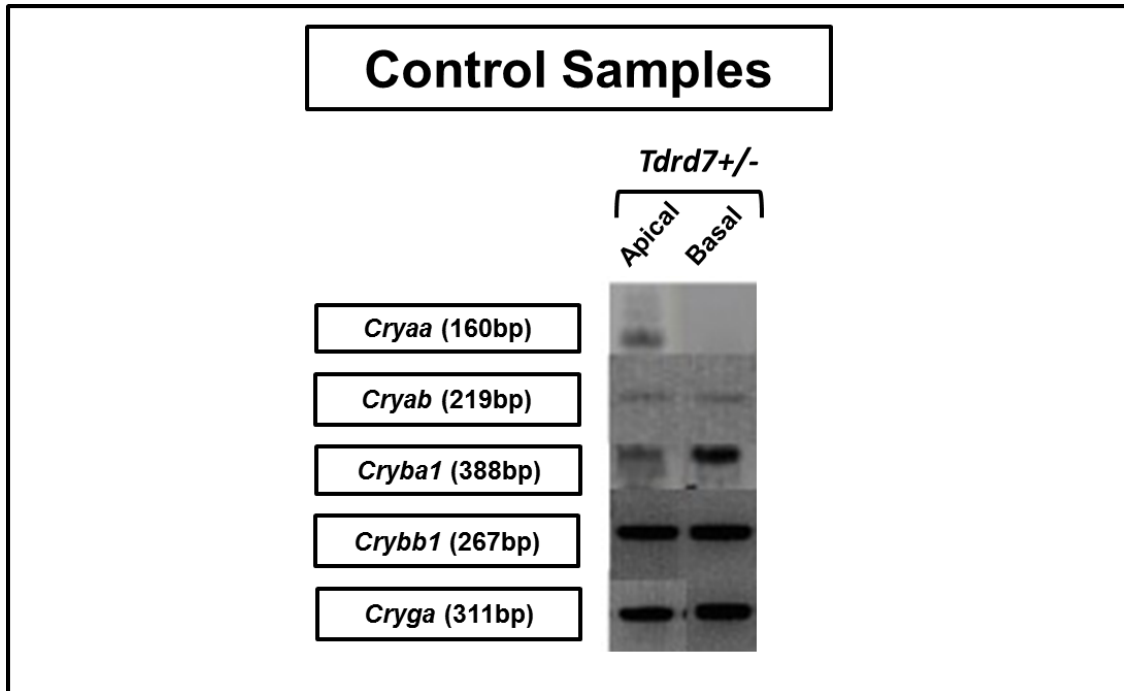


Figure 15: Heterozygous apical and basal samples were tested for *Cryaa*, *Cryab*, *Cryba1*, *Crybb1*, and, *Cryga*. *Cryaa* was found to be expressed at higher levels in the apical region of the *Tdrd7* heterozygous lens fiber cells compared to the basal region. *Cryab*, *Cryba1*, *Crybb1*, and, *Cryga* were found to be expressed at comparable levels in both, apical and basal regions of the *Tdrd7* heterozygous lens fiber cells.

Chapter 4

Discussion

TDRD7 is a Tudor family protein that is involved in the regulation of various aspects of mRNA control. At least one aspect of TDRD7 function may be mediated through its being an RNA granule component that is highly enriched in the developing chicken and mouse lens. It also associates at variable extents with other types of lens RGs known as PBs, which are involved in microRNA mediated silencing, nonsense-mediated decay (NMD), and with enzymes involved in mRNA decay process [31]. Along with PBs, TDRD7 is also associated with other cytoplasmic RNPs that contain a well-characterized RG component, Staufen1 ribonucleoproteins (STAU1 RNPs). STAU1 is a double stranded RNA binding protein [36-38] that is involved in RNA transport. Since TDRD7 colocalizes with STAU1, it was hypothesized that TDRD7 may be involved in actively transporting RNA in elongating fiber cells. Therefore, to determine if there were mRNAs that were differentially localized in apical or basal lens fiber cells and if these mRNAs were affected in *Tdrd7* null mutant lens, I tested the localization of select lens markers in the apical and basal regions of fiber cells collected from these animals by Laser Capture Microdissection (LCM) at E12.5.

To begin the project, mice were bred in a way that maximum number of mutants could be obtained. *Tdrd7* heterozygous males were bred with *Tdrd7* null females, as *Tdrd7* null males were sterile. One of the techniques that could be improved from the present study is the speed of

dissection that could be optimized to reduce the amount of RNA degradation. The dissection can also be limited to one per day to decrease the variation of time in each female's staged embryos.

My study provided evidence that lens tissue can be captured by LCM from specific regions of fiber cells. Furthermore, I demonstrated that LCM captured tissue was in sufficient quantities to prepare RNA. However, the RNA quantities obtained varied between individual samples with the concentrations of RNA ranging from 1.7 ng/ μ l to 17.6 ng/ μ l. Considering LCM is a difficult technique in itself, and the RNA was isolated from two different areas of a tissue that is less than 400 μ m wide, it may be possible to increase yield by collecting higher amounts of tissue. Although the concentrations of RNA were greater than expected, unfortunately, it was not estimated to be high enough to perform a global analysis of gene expression using tools such as microarray or RNA sequencing. However, this study also successfully demonstrated that the extracted RNA can be used for cDNA synthesis using the iScript cDNA Synthesis Kit, with the concentrations for individual samples ranging from 1,000 to 1,200 ng/ μ l and no protein contamination. In future, whether collecting E12.5 or other embryonic stages, the number of samples collected would need to be increased for preparing higher quantity RNA.

To validate the tissue samples were in fact collected from the apical and basal regions of the E12.5 lens fiber cells, the collected cDNA was used in RT-PCRs. The RT-PCRs proved to be challenging and after various different PCR conditions were tried, an optimal protocol was established for each lens marker tested. The different parameters that were changed for optimal PCR conditions were: primer concentration, cDNA quantity, MgCl₂ concentration, and primer annealing temperatures. The final thermal cycler program conditions in which the RT-PCRs worked was with annealing temperatures ranging from 47°C-57°C. Seventeen different primers were used to validate the results, as shown in Table 1.

A housekeeping gene is considered to be a constitutively expressed gene that is required for the maintenance of basic cellular function, and is found in all cell types of an organism. Various housekeeping genes can therefore be used as a reference of the overall gene expression within each cell type. The housekeeping marker, *Gapdh* was used as the reference in the RT-PCR experiments, and was found to be expressed equally in all the regions of the lens fiber cell collected tissue. This expression was used as the reference of expression for all of the genes tested.

E-cadherin, a marker for lens epithelial cells (LEC) was used to determine if the apical and basal fiber cell sections contained epithelial cell contamination. Lens epithelial cells from maintained cell lines were used as positive controls against the apical and basal fiber cell biological replicates. Positive bands were found in the maintained epithelial cell lines, whereas no bands were seen in the apical and basal fiber cell regions. This confirmed that the apical and basal regions were free from epithelial cell contamination. Another lens epithelial marker, *Foxe3*, was found to be present in all the regions of the lens fiber cell regions collected. One of the reasons why *Foxe3* was present in the fiber cell regions could be because the fiber cells may not have completely down-regulated *Foxe3* by E12.5. Furthermore we decided to test another epithelial marker, *Htra3*, and found no bands, which again confirms no contamination of epithelial tissue was detected in either the apical or basal fiber cell regions.

In addition to these markers, other well-characterized lens marker genes were tested for differential expression of these mRNA in the apical versus basal regions of the *Tdrd7* heterozygous lens fiber cells. Specifically, *Cryaa*, *Cryab*, *Cryba1*, *Cybb1* and *Cryga* were confirmed to be present in the lens fiber cells at E12.5. Interestingly, *Cryaa* was found to be

enriched in the apical region of fiber cells at this stage while other crystalline mRNA tested were found to be at similar levels in both regions.

Three additional lens fiber cell markers, *Prox1*, *Trpm3*, and *Pax6* were used to support the purity of LCM captured tissue to be of fiber cell origin. Although it was expressed in fiber cells, *Trpm3* and *Pax6* showed variations in expression levels and therefore were left out of the final analysis due to limitation of time for troubleshooting it at different conditions. *Prox1* was expressed uniformly in all the regions of the *Tdrd7*^{+/-} lens fiber cells. The expression in the *Tdrd7* null basal regions of the lens fiber cells was lower compared to *Tdrd7*^{+/-} basal regions. In future, a real time quantitative (q)RT-PCR analysis can be used to validate these observations.

Big picture conclusion:

These data demonstrate for the first time that it is feasible to use LCM to capture different regions of a single type of cell, here lens fiber cells. Furthermore, it also demonstrated that the tissue could be captured in enough quantity so as to make cDNA for analysis by RT-PCR. Purity of these samples was established by the study of various marker genes.

Future work:

Scale-up and modifications of these protocols will enable high throughput analysis of localized gene expression in lens fiber cells.

REFERENCE

1. Bhat, S.P., *The ocular lens epithelium*. Biosci Rep, 2001. **21**(4): p. 537-63.
2. Piatigorsky, J., *Lens differentiation in vertebrates. A review of cellular and molecular features*. Differentiation, 1981. **19**(3): p. 134-53.
3. Li, Y. and J. Piatigorsky, *Targeted deletion of Dicer disrupts lens morphogenesis, corneal epithelium stratification, and whole eye development*. Dev Dyn, 2009. **238**(9): p. 2388-400.
4. Gwon, A., *Lens regeneration in mammals: a review*. Surv Ophthalmol, 2006. **51**(1): p. 51-62.
5. Sue Menko, A., *Lens epithelial cell differentiation*. Exp Eye Res, 2002. **75**(5): p. 485-90.
6. Shiels, A., T.M. Bennett, and J.F. Hejtmancik, *Cat-Map: putting cataract on the map*. Mol Vis, 2010. **16**: p. 2007-15.
7. Hejtmancik, J.F., *Congenital cataracts and their molecular genetics*. Semin Cell Dev Biol, 2008. **19**(2): p. 134-49.
8. Graw, J., *Mouse models of cataract*. J Genet, 2009. **88**(4): p. 469-86.
9. Resnikoff, S., et al., *Global data on visual impairment in the year 2002*. Bull World Health Organ, 2004. **82**(11): p. 844-51.
10. Eagleson, G., B. Ferreiro, and W.A. Harris, *Fate of the anterior neural ridge and the morphogenesis of the Xenopus forebrain*. J Neurobiol, 1995. **28**(2): p. 146-58.
11. Varga, Z.M., J. Wegner, and M. Westerfield, *Anterior movement of ventral diencephalic precursors separates the primordial eye field in the neural plate and requires cyclops*. Development, 1999. **126**(24): p. 5533-46.
12. Fernández-Garre, P., et al., *A neural plate fate map at stage HH4 in the chick: methodology and preliminary data*. Brain Res Bull, 2002. **57**(3-4): p. 293-5.
13. Zuber, M.E., et al., *Specification of the vertebrate eye by a network of eye field transcription factors*. Development, 2003. **130**(21): p. 5155-67.
14. Macdonald, R., et al., *Midline signalling is required for Pax gene regulation and patterning of the eyes*. Development, 1995. **121**(10): p. 3267-78.
15. Lovicu, F.J., *Cell signaling in lens development*. Semin Cell Dev Biol, 2006. **17**(6): p. 675.
16. Robinson, M.L., *An essential role for FGF receptor signaling in lens development*. Semin Cell Dev Biol, 2006. **17**(6): p. 726-40.
17. Iyengar, L., et al., *Growth factors involved in aqueous humour-induced lens cell proliferation*. Growth Factors, 2009. **27**(1): p. 50-62.
18. Bassnett, S., *Lens organelle degradation*. Exp Eye Res, 2002. **74**(1): p. 1-6.
19. Bassnett, S., *Fiber cell denucleation in the primate lens*. Invest Ophthalmol Vis Sci, 1997. **38**(9): p. 1678-87.
20. Bassnett, S., *On the mechanism of organelle degradation in the vertebrate lens*. Exp Eye Res, 2009. **88**(2): p. 133-9.

21. Andley, U.P., *Crystallins in the eye: Function and pathology*. Prog Retin Eye Res, 2007. **26**(1): p. 78-98.
22. Blixt, A., et al., *A forkhead gene, FoxE3, is essential for lens epithelial proliferation and closure of the lens vesicle*. Genes Dev, 2000. **14**(2): p. 245-54.
23. Wigle, J.T., et al., *Prox1 function is crucial for mouse lens-fibre elongation*. Nat Genet, 1999. **21**(3): p. 318-22.
24. Medina-Martinez, O., et al., *Severe defects in proliferation and differentiation of lens cells in Foxe3 null mice*. Mol Cell Biol, 2005. **25**(20): p. 8854-63.
25. Landgren, H., A. Blixt, and P. Carlsson, *Persistent FoxE3 expression blocks cytoskeletal remodeling and organelle degradation during lens fiber differentiation*. Invest Ophthalmol Vis Sci, 2008. **49**(10): p. 4269-77.
26. Lachke, S.A., et al., *iSyTE: integrated Systems Tool for Eye gene discovery*. Invest Ophthalmol Vis Sci, 2012. **53**(3): p. 1617-27.
27. Lachke, S.A., et al., *Mutations in the RNA granule component TDRD7 cause cataract and glaucoma*. Science, 2011. **331**(6024): p. 1571-6.
28. Ponting, C.P., *Tudor domains in proteins that interact with RNA*. Trends Biochem Sci, 1997. **22**(2): p. 51-2.
29. Tanaka, T., et al., *Tudor domain containing 7 (Tdrd7) is essential for dynamic ribonucleoprotein (RNP) remodeling of chromatoid bodies during spermatogenesis*. Proc Natl Acad Sci U S A, 2011. **108**(26): p. 10579-84.
30. Pek, J.W., A. Anand, and T. Kai, *Tudor domain proteins in development*. Development, 2012. **139**(13): p. 2255-66.
31. Parker, R. and U. Sheth, *P bodies and the control of mRNA translation and degradation*. Mol Cell, 2007. **25**(5): p. 635-46.
32. Anderson, P. and N. Kedersha, *Stress granules*. Curr Biol, 2009. **19**(10): p. R397-8.
33. Buchan, J.R. and R. Parker, *Eukaryotic stress granules: the ins and outs of translation*. Mol Cell, 2009. **36**(6): p. 932-41.
34. Thomas, M.G., et al., *RNA granules: the good, the bad and the ugly*. Cell Signal, 2011. **23**(2): p. 324-34.
35. Ohn, T., et al., *A functional RNAi screen links O-GlcNAc modification of ribosomal proteins to stress granule and processing body assembly*. Nat Cell Biol, 2008. **10**(10): p. 1224-31.
36. Roegiers, F. and Y.N. Jan, *Staufen: a common component of mRNA transport in oocytes and neurons?* Trends Cell Biol, 2000. **10**(6): p. 220-4.
37. Furic, L., M. Maher-Laporte, and L. DesGroseillers, *A genome-wide approach identifies distinct but overlapping subsets of cellular mRNAs associated with Staufen1- and Staufen2-containing ribonucleoprotein complexes*. RNA, 2008. **14**(2): p. 324-35.
38. Vessey, J.P., et al., *A loss of function allele for murine Staufen1 leads to impairment of dendritic Staufen1-RNP delivery and dendritic spine morphogenesis*. Proc Natl Acad Sci U S A, 2008. **105**(42): p. 16374-9.
39. Gong, C. and L.E. Maquat, *lncRNAs transactivate STAU1-mediated mRNA decay by duplexing with 3' UTRs via Alu elements*. Nature, 2011. **470**(7333): p. 284-8.
40. Pontoriero, G.F., et al., *Co-operative roles for E-cadherin and N-cadherin during lens vesicle separation and lens epithelial cell survival*. Dev Biol, 2009. **326**(2): p. 403-17.
41. Shaham, O., et al., *Pax6 is essential for lens fiber cell differentiation*. Development, 2009. **136**(15): p. 2567-78.

42. Hung, G. K. (2001), *Models of Oculomotor Control*. River Edge, World Scientific Publishing Co.
43. Modified from: Dr. Richlin, O.D. & Associates, Eye conditions library.
44. K. Krishna Sharma and Puttur Santhoshkumar, *Lens aging: effects of crystallins*, 2009.
45. Oyster, C. (1999). *The Lens and the Vitreous. The Human Eye: Structure and Function*. Sunderland, Sinauer Associates, Inc.: 491-544
46. Modified from Kuszak & Brown, 1994 (Image).
47. The eye Practice, Sydney.
48. Developmental Biology 2005.
49. Summary by Moormann et al., 1982